Generalization of the Fahraeus principle for microvessel networks

A. R. PRIES, K. LEY, AND P. GAEHTGENS
Department of Physiology, Freie Universität Berlin, D-1000 Berlin 33, Federal Republic of Germany

PRIES, A. R., K. LEY, AND P. GAEHTGENS. *Generalization of the Fahraeus principle for microvessel networks.* Am. J. Physiol. 251 (Heart Circ. Physiol. 20): H1324–H1332, 1986.—Microvessel hematocrits and diameters were determined in each vessel segment between bifurcations of three complete microvascular networks in rat mesentery. Classification of the segments as arteriolar, venular, or arteriovenular (av) was based on flow direction at branch points. Photographic and videomicroscopic mapping was used to obtain quantitative information on the architecture and topology of the networks. This topological information allowed the analysis of hematocrit distribution within a series of consecutive-flow cross sections, each of which carried the total flow through the network. The observed reduction of mean hematocrit in the more peripheral cross sections is explained by the presence of a "vessel" and a "network" Fahraeus effect. The vessel Fahraeus effect results from velocity difference between red cells and blood within the individual vessel segments due to the existing velocity and cell concentration profiles. The network Fahraeus effect is based on the velocity difference of red cells and blood caused by velocity and hematocrit heterogeneity between the vessels constituting any of the complete-flow cross sections. The network Fahraeus effect is found to account for ~20% of the total hematocrit reduction and increases toward the most distal cross sections.

Fahraeus effect; rat mesentery; intravital microscopy; tube hematocrit; discharge hematocrit

VERY LOW VALUES of capillary hematocrit have been reported for cat mesentery (2, 6), rabbit omentum (28), hamster cremaster muscle (19), rat mesentery (18), and rat cremaster muscle (15). In these studies the fractional volume occupied by red cells in microvessels (H_T or H_{micro}) was determined, and mean values at the capillary level were found to range between 20 and 48% of systemic hematocrit.

Since H_T reflects the fractional volume of erythrocytes actually contained within a microvessel, it is an important determinant of microvascular flow resistance. On the other hand, the amount of O_2 delivered to the tissue is a function of the flow fraction of red cells, known as discharge hematocrit (H_D).

In microvessels with diameters below ~100 μm, H_T is always lower than H_D, since the average red cell velocity is higher than the mean blood velocity (1–3). This phenomenon was first described by Fahraeus (7). The theoretical lower limit of the ratio H_T/H_D in tubes with circular or elliptical cross section is 0.5 (3). The experimentally observed minimum ratio H_T/H_D for discharge hematocrits between 0.3 and 0.4 averaged 0.65 and was seen in tubes of ~10- to 20-μm diam (1, 2, 9, 10). Therefore, the hematocrit reduction observed in the aforementioned studies in vivo cannot be attributed to the Fahraeus effect alone and additional mechanisms must be considered.

It has been suggested that the low values of H_T determined in microvessels are partially due to a hypothetical stationary plasmatic zone close to the wall of these vessels (19). A similar effect could result from an irregular shape of the vessel cross section. In both cases the lower limit of H_T/H_D would be <0.5.

Second, capillary hematocrit could be affected by fluid transport across the microvessel wall. However, it is known from studies in different organs (22) that the fluid transport rates are generally too small to influence capillary hematocrit. Also filtration exceeds reabsorption in most tissues and would therefore lead to an increase of capillary hematocrit compared with systemic rather than the observed decrease.

A third candidate for a modulation of mean microvascular hematocrit is the heterogeneous distribution of flow within microvascular networks. It is known from in vitro investigations (4, 6, 8, 24, 31) that hematocrit distribution at branch points is affected by the volume flow distribution due to plasma skimming and red cell screening effects: at a bifurcation, the daughter vessel with higher flow rate receives an elevated hematocrit compared with the parent vessel, and vice versa. Some in vivo studies (17, 20, 25, 27) suggest that such separation effects are also present at microvascular bifurcations.

In a network of microvessels this phase separation effect would occur at many consecutive arteriolar bifurcations. Conservation of red cell and blood volume flow requires that the increase of hematocrit in the high-flow branch must be smaller than the decrease of hematocrit in the low flow branch. This would reduce the mean hematocrit at the capillary level (5, 18, 23). In the present study an attempt was made to improve the interpretation of the observed hematocrit distribution by collecting complete data sets for entire microvascular networks and relating them to the existing network structure. This requires that the individual vessels are not categorized according to morphological parameters, such as diameter, but according to their topological position within the network.

0363-6135/86 $1.50

MATERIALS AND METHODS

Male Wistar rats (body wt 300–450 g) were anesthetized with pentobarbital sodium (60 mg/kg sc). Trachea, left carotid artery, and jugular vein were cannulated, and mean arterial pressure, heart rate, and central venous pressure were monitored continuously.

After abdominal midline incision, the mesentery was cautiously spread over the glass pedicle of an appropriate stage. The preparation was superfused with a thermostated (36.5°C) bicarbonate-buffered saline solution, which was kept at a low Po_2 and a pH of 7.4 by continuous bubbling with 5% CO_2 in N_2. Systemic hematocrit (H_{sys}) was determined repeatedly by centrifugation of carotid blood samples. The values ranged from 0.46 to 0.50. Mean corpuscular volume was determined by additional blood cell counting and was found to average 56 μm^3.

The mesenteric microcirculation was observed under transillumination with monochromatic blue light (xenon arc lamp or flash, BG 12 filter, small-band interference filter 448 nm) on a Leitz intravital microscope (Fig. 1*A*). The microscope was modified according to the principles of telescopic imaging (29). The registration equipment, a multidiode silicon target video camera (RCA 1005) and a motor-driven photo camera (Olympus OM 2), was positioned on a separate mounting plane above the microscope. With a ×25 water-immersion objective (Leitz SW 25/0.60), the total magnification on the target of the video camera was ~×28.

An area of the mesentery of ~25 mm^2 was scanned in ~20 min. These areas were chosen such that no fat tissue was included and all blood vessels from the largest feeding arterioles to the draining venules could be observed. Each field of view was recorded both on video tape under continuous illumination and on negative film (Kodak Panatomic 32 ASA) using flash illumination. From the photographic recordings a photomontage consisting of ~100 prints was assembled (Fig. 2).

The vessels of the mesenteric network were classified on the basis of the flow direction as determined from the video recordings: any vessel segment linked to the feeding arteriole of the network by divergent bifurcations and itself connecting two divergent bifurcations was called arteriolar, any one linked to the venous outflow by convergent bifurcations and connecting two convergent bifurcations was called venular. The segments connecting the arteriolar to the venous vessel tree were denominated arteriovenular (av) vessel segments. In the mesenteric networks studied here most arteriovenous connections consist of a single av vessel segment; only in 5% of the av pathways is a mesh found. In these cases only the av segments closest to the arterial inflow were included in the analysis, and the subsequent branching was ignored. An ambiguity of this nomenclature could result from the occurrence of flow reversal, which was, however, only seen in one vessel segment within the period of observation.

A generation number was assigned to any microvascular segment, starting with 1, for the main feeding arteriole and draining venule, respectively, and adding 1 at each node (Fig. 3). The highest generation number for the most peripheral av segment in the largest network investigated so far was 20. Figure 3 also shows the widely applied Horton-Strahler ordering scheme (14, 30). This scheme was not used in the present study, because not all vessels of a given Strahler order are connected in series to those of the next higher order. Therefore, this scheme is not suitable for mass conservation considerations. The properties of different nomenclatures applied to the microcirculation are discussed in detail elsewhere (11). For each microvascular segment vessel diameters were measured from the photo negatives to take advantage of the higher resolution of the film compared with the video system. From the video recordings microvascular hematocrit was determined in all vessel segments within the scanned area using a microphotometric method described in detail elsewhere (26). This method was calibrated for tube and discharge hematocrits in the range from 0.05 to 0.80 for vessel diameters ranging from 8 to 60 μm. In the calibration procedure glass tubes within this diameter range were perfused with red blood cell suspensions of known hematocrit (H_D). The corresponding H_T were calculated from H_D using data on the Fahraeus effect for rat blood previously determined in tubes of similar size (26).

The optical density of the perfused tubes was measured and correlated to the discharge and to the tube hematocrit. Two empirical calibration equations were obtained that allow the conversion of optical density to H_T and H_D. These equations are given in the APPENDIX.

Since it is H_T rather than H_D that determines the measured optical density, the method is only valid for determination of H_D in vivo if the Fahraeus effect (ratio H_T/H_D) is similar in glass tubes and microvessels.

Optical density was measured as the difference in light intensities on the microvessel and on the black reference divided by the difference between the surrounding tissue and the black reference (Fig. 1*B*). The light intensities were derived from the BAS signal of the video camera by using a videodensitometer (IPM, San Diego).

In vessels with diameters below 10 μm an attempt was made to count red cells per unit vessel length on the projected photographs. Whenever this was possible these data were converted into H_T using the independently determined mean red cell volume and into H_D using the established data on Fahraeus effect in tube flow (1, 26). Results of this approach were preferred to the values determined by microphotometry.

RESULTS

The total number of microvessel segments in the three microvascular networks studied was 1,303. In a complete, dichotomous network fed and drained by just one vessel, the number of arteriolar and venular segments should theoretically be equal and the number of av segments should be higher by one. In the material presented here the number of av segments was slightly smaller (by 6%) than that of the arteriolar and venular segments because the networks were not strictly self contained and the feeding and draining vessel of the network was not the only vessel entering or leaving the scanned area of the mesentery.

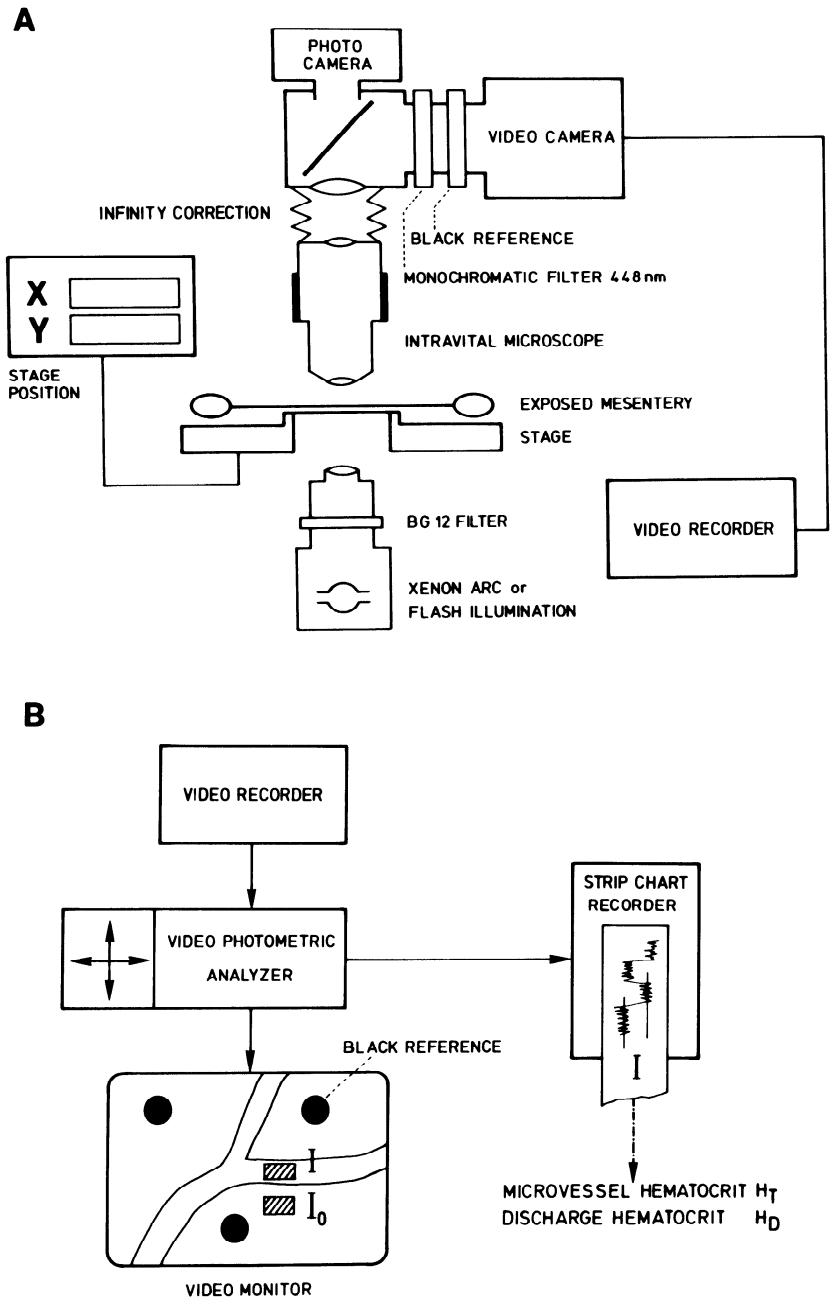

FIG. 1. *A*: schematic drawing of experimental setup. *B*: off-line determination of microvessel hematocrit (H_T) and discharge hematocrit (H_D). By use of adjustable cursors of videophotometric analyzer (*hatched rectangles* on video monitor) light intensity differences I and I_o were measured and recorded on a strip-chart recorder. These values together with vessel diameter served to calculate H_T and H_D.

Figure 4 shows the diameter distribution of all arteriolar, arteriovenular, and venular vessel segments constituting the networks analyzed. All distributions exhibit a significant skewness; arteriolar diameters range between 5 and 43 μm, venular diameters between 8 and 60 μm. As shown by Fig. 4, the diameters of the av segments as defined here vary over a fourfold range from 5 to 22 μm.

The hematocrit measurements are presented in Fig. 5 in the conventional form by plotting hematocrit versus vessel segment diameter. The upper panels show an increase of tube hematocrit with microvessel diameter; this is more apparent from the calculated mean values shown in the middle row. In the diameter range above 40 μm the venular segments seem to show a reduction of hematocrit with increasing diameter. This may be due to a systematic error of hematocrit measurements caused by an elliptic cross section of these vessels. In all three vessel categories the range of hematocrit values increases with decreasing vessel diameter. The coefficient of variation, which is independent of increasing sample size, also increases with decreasing vessel diameter (middle row). The solid lines in the top and bottom panels separate the group of vessel segments in which the discharge hematocrit is lower than H_{sys} from those in which H_D exceeds H_{sys}. In the upper panels these lines are calculated using in vitro measurements of the Fahraeus effect (26). In the diameter range below 20 μm the majority of data points fall below these lines.

Since information on network topology is available in the present study along with the hematocrit data for each vessel segment present in the scanned field it is possible to define "complete flow cross sections" that carry the total inflow of the network. A complete flow cross section is defined as a group of vessel segments selected such

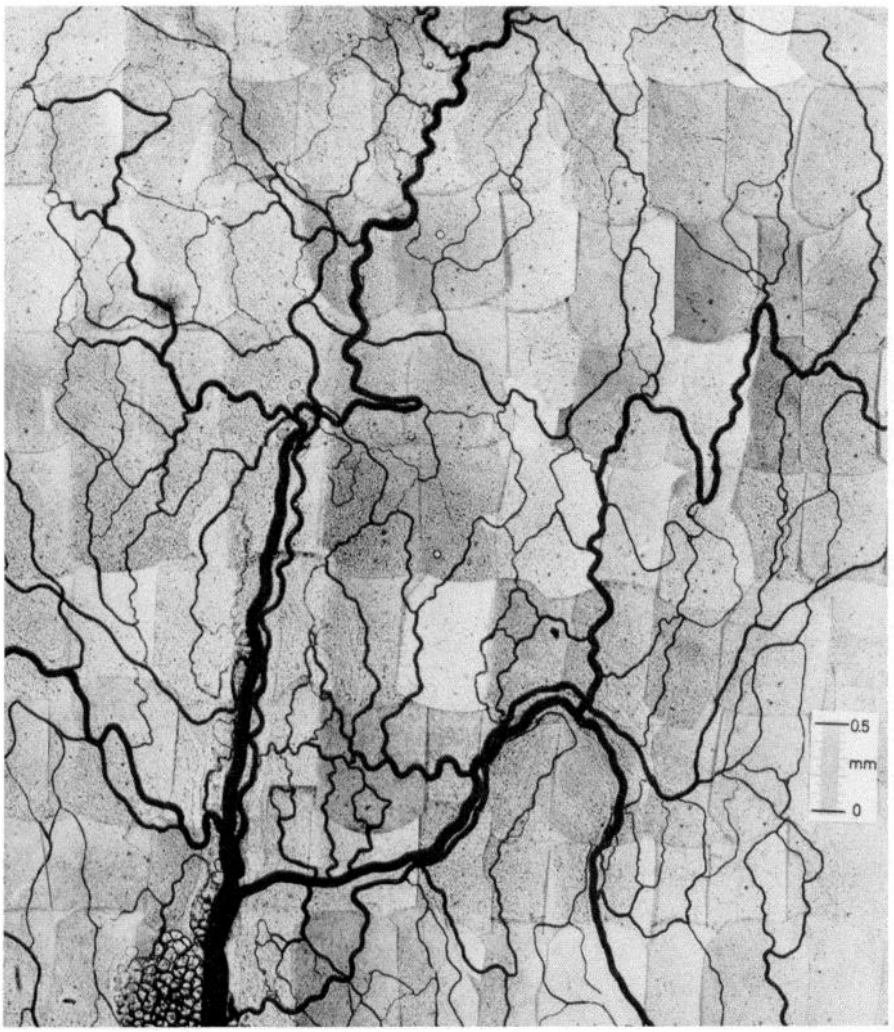

FIG. 2. Photomontage of a mesenteric microvessel network with an area of ~31 mm^2 recorded in ~100 single fields of view.

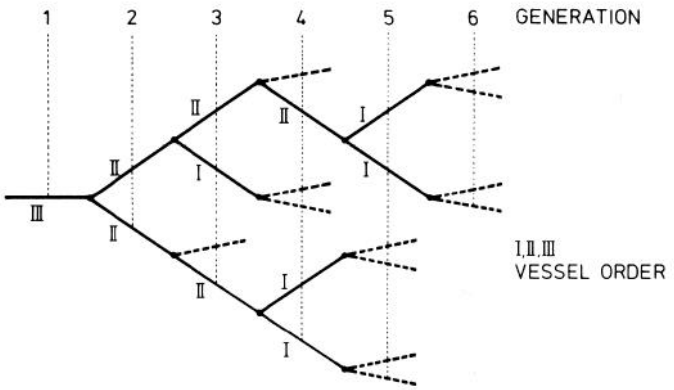

FIG. 3. Numbering schemes for vessel segments (*dashed lines*: arteriovenular segments). *Arabic numerals* refer to generation numbering used in present study. This centrifugal scheme starts with *number 1* at inflow (or outflow) vessel. Generation number increases by one at each bifurcation. *Roman numerals* illustrate centripetal Horton-Strahler ordering scheme.

that each fluid element of the blood traversing the network passes precisely one of the vessel segments in this group on its way from the feeding arteriole to the collecting venule. Obvious complete flow cross sections are, for instance, the arteriole feeding the network or the group of av segments. Figure 6 depicts in a schematic way a number of complete flow cross sections that can be generated in a given microvessel network. Each of these flow cross sections contains the arteriolar and av segments of a given generation "X" plus all av segments with lower generation numbers. This is called "complete flow cross section at generation level X."

The four panels of Fig. 7 show the frequency distributions of normalized discharge hematocrit (H_D/H_{sys}) for the complete flow cross sections at the generation levels 5, 10, 15, and 20 (av segments). These histograms were obtained from pooled data of three mesenteric networks. Here and in the following analysis minor inflow arterioles and their offsprings have been disregarded so that each of the networks considered is fed by only one arteriole. For these networks the mean H_D/H_{sys} is 0.87 at the generation level 1 (inflow vessels). With increasing generation number the mean H_D/H_{sys} decreases and the coefficient of variation increases.

DISCUSSION

A low level of microvascular hematocrit is suggested by indicator-dilution studies that have shown whole body

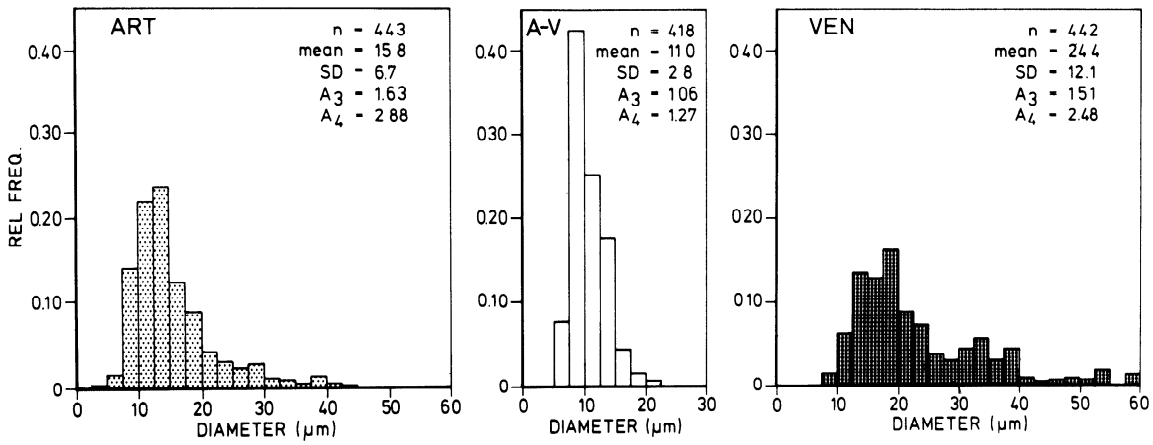

FIG. 4. Frequency distributions of diameters of arteriolar (ART), arteriovenular (av), and venular (VEN) segments for combined data of 3 microvessel networks. In each panel number of segments (n), mean diameter, and standard deviation (SD) are given together with skewness (A_3) and kurtosis (A_4).

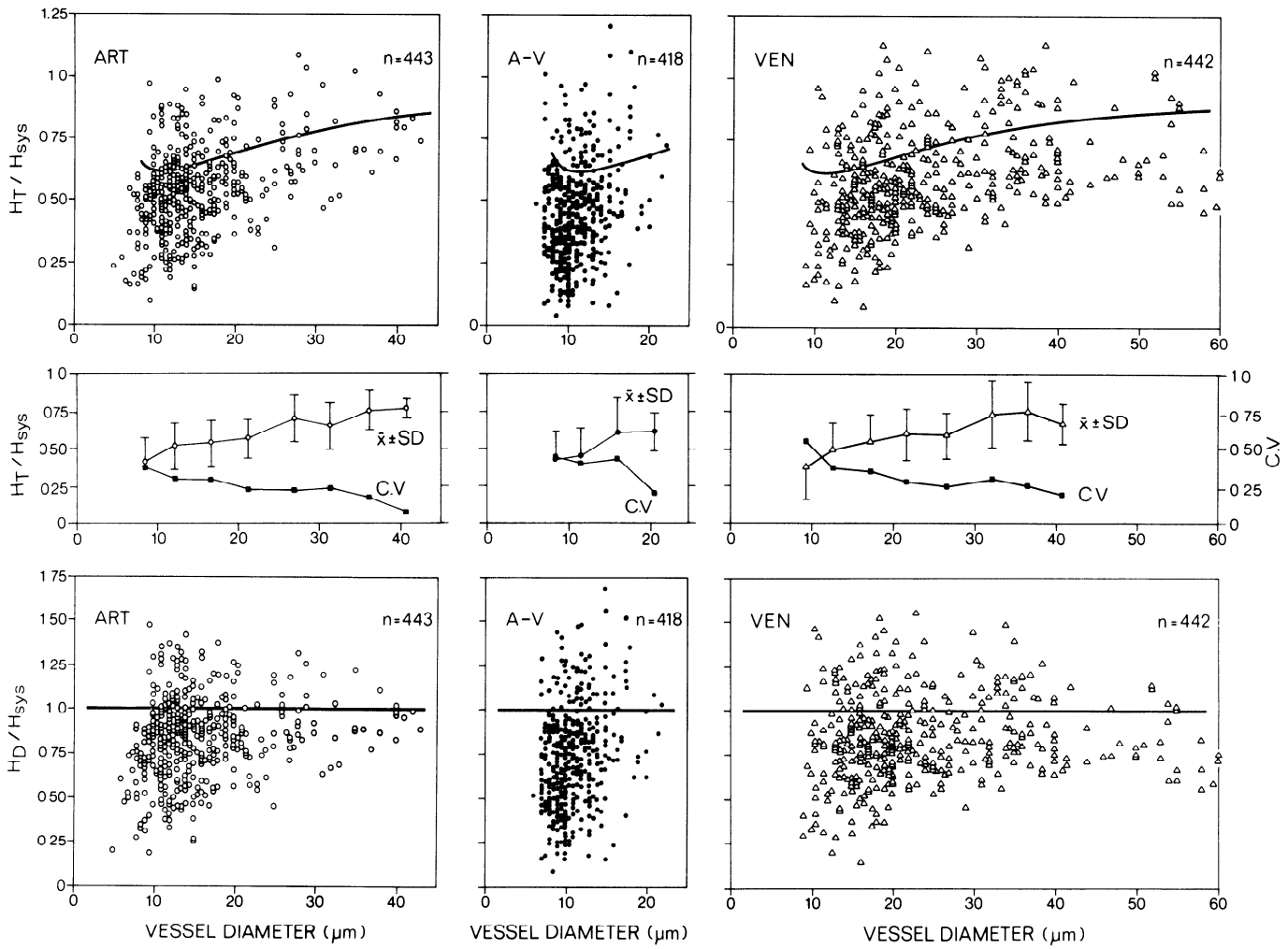

FIG. 5. Vessel segment hematocrit plotted against diameter (combined data from three networks). All hematocrits are normalized with respect to systemic hematocrit (H_{sys}). *Top panels*: normalized tube hematocrit (H_T/H_{sys}) for arteriolar (ART), arteriovenular (AV), and venular (VEN) segments. *Solid lines* represent hematocrit reduction predicted by the Fahraeus effect as measured in vitro assuming H_D equals H_{sys}. *Middle panels*: *upper lines* give mean values and standard deviations of H_T/H_{sys}. *Lower lines* give corresponding coefficients of variation (CV). *Bottom panel*: normalized discharge hematocrit H_D/H_{sys}.

hematocrit to be lower than large-vessel hematocrit (12, 13). Several intravital microscopic studies of the mesentery (16, 18, 21), and other tissues accessible to direct measurement of microvessel hematocrit (19, 28), have confirmed that microvascular hematocrit is low compared with systemic hematocrit and that there is a large variability of values in individual microvessels.

Some of these studies are based on counting the num-

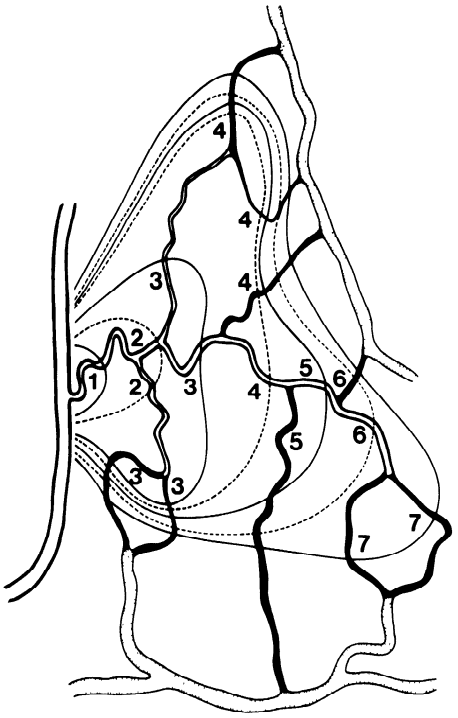

FIG. 6. Schematic drawing of a microvessel network. Arteriolar vessel segments are drawn *open*, venular segments *stippled*, arteriovenular segments *black*. *Numerals* refer to generation numbers. *Solid* and *dashed lines* indicate a series of consecutive-flow cross sections.

ber of red cells per unit capillary volume and computing H_T using mean red cell volume (16, 19, 28). In these studies H_T in larger vessels could not be analyzed because of overlapping cells (multifile flow). Other studies made use of microphotometric methods for hematocrit determination in vessels in which single red cells are not discernible (15, 18, 21).

In these studies vessels were selected for measurement of hematocrit and categorized according to morphological criteria, mostly diameter. Apart from a possible bias introduced by the selection process it was impossible to analyze the obtained data in relation to the branching structure of the microvascular network.

The definition of complete flow cross sections using the generation numbering scheme allows the application of mass conservation considerations to observed hematocrit distributions. The data show a progressive reduction of mean discharge hematocrit from the inflow generation to the cross section of av segments (Fig. 7). This confirms, on one hand, that the classical Fahraeus effect in the single vessel elements does not suffice to explain the experimental findings. On the other hand, it must be questioned whether the arithmetic mean of the discharge hematocrits in the individual vessel segments in any complete flow cross section is a correct representation of the average ratio between red cell and blood flow through this cross section.

Several authors have shown theoretically that a heterogeneous distribution of blood flow within a network can lead to a reduction of mean H_D compared with the inflow hematocrit if it is combined with a heterogeneous distribution of vessel hematocrit (5, 18, 23): a reduction of mean discharge hematocrit at a given flow cross section is to be expected if phase separation at the preceding bifurcations of the network leads to higher hematocrits in the faster flowing vessels.

Fahraeus (7) pointed out that in single vessels H_T is lower than H_D by a factor that is identical to the velocity ratio v_b/v_c[1]

$$H_T = H_D \cdot \frac{v_b}{v_c} \qquad (1)$$

[1] It must be stated that the velocity values used here are defined as arithmetic means of the velocities of fluid elements contained in a vessel of a given length at a given time instant. The common way to determine mean cell velocities, however, is to average the velocities of all cells passing a point of observation in a certain time interval. Since velocity is a ratio of length over time, this average value is not a correct representation of the mean velocity of the observed cells. If such a measuring protocol is used, the harmonic mean yields a correct value of mean red cell velocity.

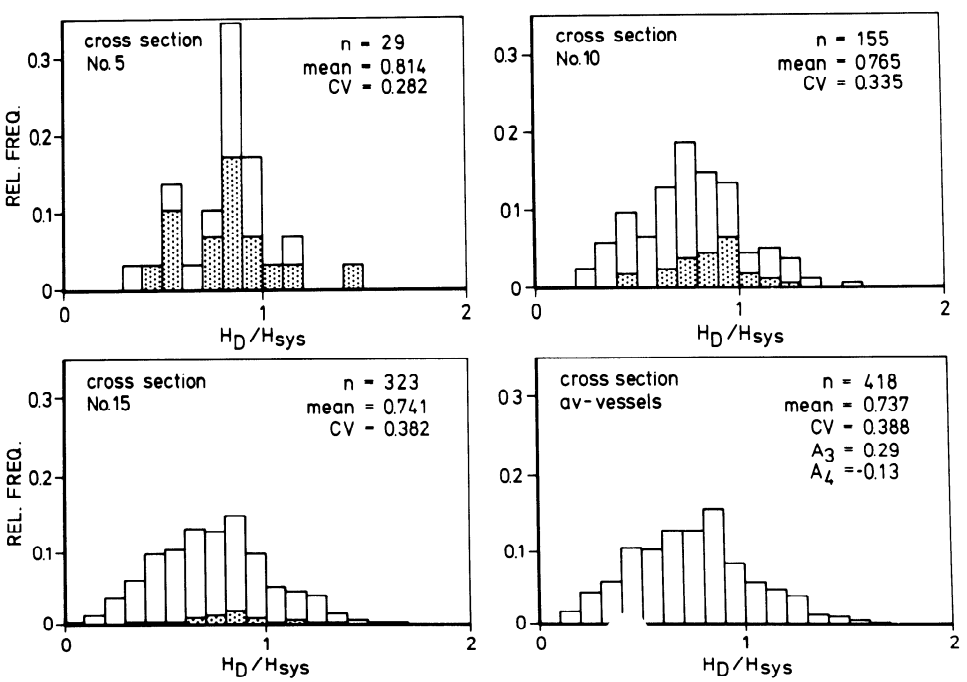

FIG. 7. Frequency distribution of normalized discharge hematocrit (H_D/H_{sys}) at 4 complete-flow cross sections. Each *panel* lists number (n) of vessel segments, mean value, and coefficient of variance (CV) of H_D/H_{sys}. Skewness (A_3) and kurtosis (A_4) are indicated for arteriovenular cross section. *Stippled parts* of *columns* indicate fraction of arteriolar segments, *open parts* represent fraction of arteriovenular segments within each cross section.

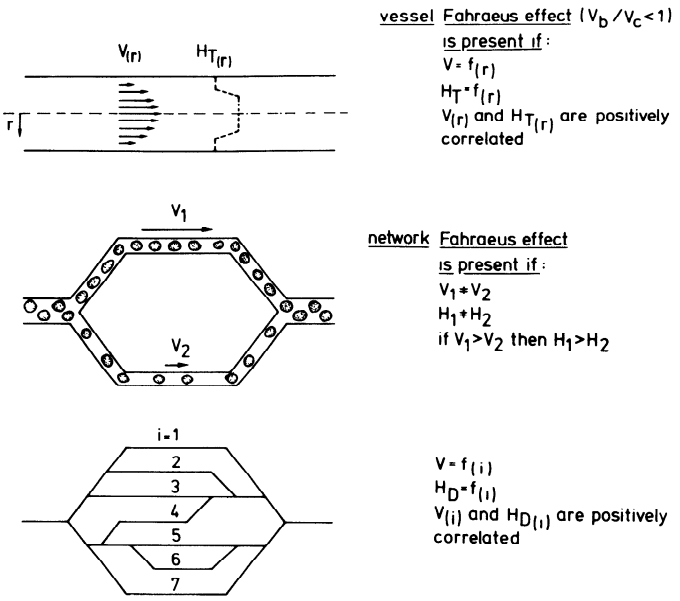

FIG. 8. Schematic representation of set of conditions for presence of vessel and network Fahraeus effects.

As illustrated in Fig. 8 (top panel) this hematocrit reduction is based on three prerequisites: *1*) the existence of a velocity profile across the vessel; *2*) a profile of tube hematocrit, and *3*) a positive correlation between these profiles. If these prerequisites are fulfilled, the red cells will travel faster through the vessel than the blood; for the purpose of the present discussion, this will be called "vessel Fahraeus effect", and the corresponding velocity ratio is denominated VF.

An isomorphic set of conditions can be defined for a number of microvessels constituting a complete flow cross section within a microvascular network (Fig. 8). Assume *1*) that a difference in flow velocity exists between these vessels, and *2*) the discharge hematocrit in these vessels varies as a result of upstream phase separation. If furthermore *3*) velocities and discharge hematocrits of the different vessels are positively correlated, the mean velocity of red cells transported through the vessels constituting the flow cross section will be larger than the average blood velocity. Fulfillment of these three conditions will lead to a reduction of the average discharge hematocrit of the flow cross section relative to the inflow hematocrit. We call this phenomenon "network Fahraeus effect"; the corresponding velocity ratio is denominated NF.

Although both vessel and network Fahraeus effect are due to a velocity difference between red cells and blood, the resulting hematocrit changes are of different nature: the vessel Fahraeus effect reduces the volume fraction of red cells within the vessel (tube hematocrit) compared with their flow fraction (discharge hematocrit). The network Fahraeus effect, in contrast, reduces the average discharge hematocrit of a flow cross section compared with the discharge hematocrit of the arteriole feeding the network. Whereas the hematocrit reduction due to the vessel Fahraeus effect is restricted to values between 1 and 0.5 vessels of circular or elliptical cross section, there is no such limitation for the network Fahraeus effect.

The velocity ratio between blood and red cells observed at a complete flow cross section ($\bar{v}_b/\bar{v}_c$) is a combination of the velocity ratios forming the basis of the vessel and network Fahraeus effects. According to the Fahraeus principle this velocity ratio describes the total hematocrit reduction (THR) at a complete flow cross section

$$\mathrm{THR} = \frac{\bar{v}_b}{\bar{v}_c} \tag{2}$$

To apply this concept to the present experimental data an approach was developed that allows the calculation of THR, vessel and network Fahraeus effect from known H_D, H_T, and diameters of the vessel segments constituting a complete flow cross section, since v_c and v_b are not available.

The mean blood and cell velocities on a complete flow cross section are given as

$$\bar{v}_b = \frac{\sum_{i=1}^{n} (Q_i)}{\sum_{i=1}^{n} (A_i)} = \frac{\sum_{i=1}^{n} (v_{b_i} \cdot A_i)}{\sum_{i=1}^{n} (A_i)} \tag{3}$$

and

$$\bar{v}_c = \frac{\sum_{i=1}^{n} (Q_i \cdot H_{D_i})}{\sum_{i=1}^{n} (A_i \cdot H_{T_i})} = \frac{\sum_{i=1}^{n} (v_{c_i} \cdot H_{T_i} \cdot A_i)}{\sum_{i=1}^{n} (H_{T_i} \cdot A_i)} \tag{4}$$

where Q_i is the volume flow, A_i the cross-sectional area, H_{T_i} the tube hematocrit, H_{D_i} the discharge hematocrit, v_{b_i} the blood velocity, and v_{c_i} the cell velocity of the vessel segment *i*. The sum is taken over the constituting vessel segments of the complete flow cross section. Combination of *Eqs. 3* and *4* with *Eq. 2* results in

$$\mathrm{THR} = \frac{\Sigma(v_{b_i} \cdot A_i)}{\Sigma(A_i)} \cdot \frac{\Sigma(H_{T_i} \cdot A_i)}{\Sigma(v_{c_i} \cdot H_{T_i} \cdot A_i)} \tag{5}$$

The discharge hematocrit of the arteriole feeding the network (H_D^*) is given as the volume flow of red cells (Q_c) divided by the volume flow of blood (Q_b)

$$H_D^* = \frac{Q_c}{Q_b} \tag{6}$$

According to the mass-conservation principle, Q_b and Q_c are constant over all complete flow cross sections, if there is no net fluid transport through the vessel walls. Therefore *Eq. 6* can be rewritten as

$$H_D^* = \frac{\Sigma(Q_{c_i})}{\Sigma(Q_{b_i})} = \frac{\Sigma(v_{c_i} \cdot H_{T_i} \cdot A_i)}{\Sigma(v_{b_i} \cdot A_i)} \tag{7}$$

where Q_{c_i} is the volume flow of red cells and Q_{b_i} is the volume flow of blood of the vessel segment *i*, and where the sums are again taken over all vessel segments of a complete flow cross section. Multiplication of *Eqs. 5* and *7* yields

$$\mathrm{THR} \cdot H_D^* = \frac{\Sigma(H_{T_i} \cdot A_i)}{\Sigma(A_i)} \tag{8}$$

The right side of this equation represents a mean value of the tube hematocrits of a complete flow cross section weighted by their individual cross-sectional areas $\bar{H}_T^A$. Therefore, THR is given as

$$THR = \frac{\bar{H}_T^A}{H_D^*} \quad (9)$$

If for the vessel segments of a flow cross section H_T and vessel cross-sectional area (calculated from the vessel diameter) are positively correlated as shown for the av segments in Fig. 5, $\bar{H}_T^A$ will be higher than the plain arithmetic mean of the tube hematocrits (H_T). Mass balance calculations based on H_T would therefore suggest an apparent loss of cells.

The vessel Fahraeus effect results from the velocity ratio of cells and blood within individual vessels (VF), whereas the network Fahraeus effect depends on the velocity ratio between different vessels (NF); thus both effects are physically independent. The combined effect at a complete-flow cross section (THR) is therefore given by multiplication of the velocity ratios $\overline{VF}$ and NF, where $\overline{VF}$ represents an effective mean of the vessel Fahraeus effects in the constituting vessels

$$THR = \overline{VF} \cdot NF \quad (10)$$

In the absence of vessel Fahraeus effects, $\overline{VF}$ equals unity and THR equals NF. Since in this case H_T and H_D in each vessel and therefore $\bar{H}_T^A$ and $\bar{H}_D^A$ (which is defined in analogy to $\bar{H}_T^A$) are equal, NF for a complete-flow cross section is then given as

$$NF = \frac{\bar{H}_D^A}{H_D^*} \quad (11)$$

Since vessel and network Fahraeus effects are independent of each other, *Eq. 11* can be generalized for situations where $H_T \neq H_D$ and $\overline{VF} \neq 1$. Thus the network Fahraeus effect is represented by the quotient of the mean area weighted discharge hematocrit of a complete-flow cross section and the discharge hematocrit in the feeding vessel of the network.

By combining *Eq. 11* with *Eqs. 9* and *10* $\overline{VF}$ for a given complete-flow cross section can be calculated as

$$\overline{VF} = \frac{\bar{H}_T^A}{\bar{H}_D^A} \quad (12)$$

In summarizing these deductions it can be concluded that the hematocrit reduction in the network must be represented using averages of the tube or discharge hematocrits in all vessels constituting a complete flow cross section weighted by the individual cross-sectional areas, rather than by using the plain arithmetic mean values. Only this approach allows a correct estimation of the changes of total volume fraction or total flow fraction of red cells relative to the inflow.

With the use of *Eqs. 9, 11,* and *12* the total hematocrit reduction as well as the network and the vessel Fahraeus effect can be quantified on the basis of hematocrit and diameter data for the vessels of a complete flow cross section. Figure 9 shows the results of such calculations for the combined data of three mesenteric networks. It

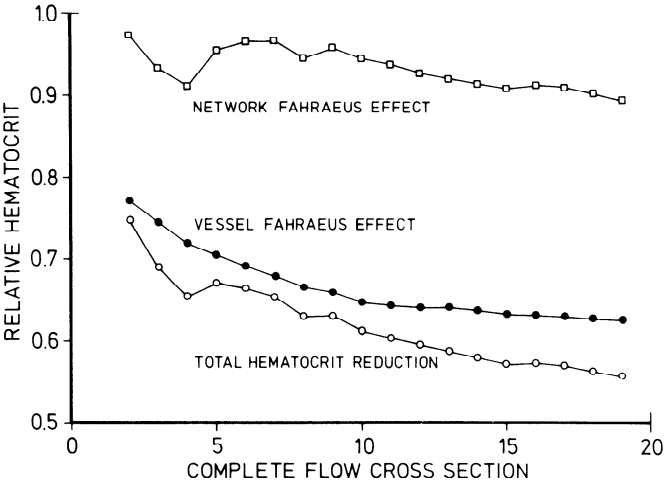

FIG. 9. Contribution of vessel and network Fahraeus effects to total hematocrit reduction for consecutive-flow cross sections in 3 mesenteric microvessel networks. Hematocrit ratio given on *ordinate* is $\bar{H}_D^A/H_D^*$ for network Fahraeus effect, $\bar{H}_T^A/\bar{H}_D^A$ for the vessel Fahraeus effect, and $\bar{H}_T^A/H_D^*$ for total hematocrit reduction.

can be seen that the vessel Fahraeus effect accounts for the major part of the total hematocrit reduction at all complete flow cross sections. In addition, it is obvious that this effect leads to a significant hematocrit reduction already in the proximal portion of the network. This is, of course, the result of the diameter dependence of red cell overvelocity (1, 2) in individual vessel segments. Figure 9 also shows that the contribution of the network Fahraeus effect to the total hematocrit reduction is relatively small. The overall trend of the data indicates an increasing contribution of the network Fahraeus effect in the more peripheral branches of the network. This is interpreted to indicate the additive effects of flow separation at consecutive branch points.

The validity of the quantitative balance between vessel and network Fahraeus effect depends on the validity of the H_T and H_D measurement. Although the H_T values reported here are comparable with data previously determined with independent methods (15, 16, 19), the H_D calibration relies on the assumption that the Fahraeus effect is the same in microvessels and glass tubes of similar size. This assumption can at present not be validated in vivo.

A systemic error in the determination of H_D would only affect the obtained relative magnitudes of vessel and network Fahraeus effect. Irrespective of this possibility, the present analytical approach represents an essential tool for the evaluation and interpretation of the hematocrit reduction in microvessel networks.

APPENDIX

In the calibration experiments that were performed with blood-perfused glass tubes according to Pries et al. (26) sets of data were obtained correlating H_T or H_D respectively to optical density (OD) for given tube diameters (ID). With the use of the empirical parameters

$$E_{H_T} = (ID - 4.74) \cdot [(1.5 + 23.83 \cdot ID^{-1.084}) \cdot H_T - H_T^2] \quad (13)$$

and

$$E_{H_D} = ID^{2.223} \cdot (302.7 \cdot ID^{-1.121} \cdot H_D - H_D^2) \quad (14)$$

these data could be fitted by linear regression lines with the equations

$$OD_{H_T} = 0.04593 \cdot E_{H_T} - 0.0102 \quad (15)$$

with $r = 0.996$, and

$$OD_{H_D} = 0.0001304 \cdot E_{H_D} - 0.01742 \quad (16)$$

with $r = 0.995$. These equations can be solved for H_T and H_D, respectively

$$H_T = \frac{23.83 \cdot ID^{-1.084} + 1.5}{2} - \left[\left(\frac{23.83 \cdot ID^{-1.084} + 1.5}{2}\right)^2 - \frac{OD + 0.0102}{0.04593(ID - 4.74)}\right]^{0.5} \quad (17)$$

$$H_D = 151.4 \cdot ID^{-1.121} - \left[(151.4 \cdot ID^{-1.121})^2 - \frac{OD + 0.01742}{0.0001304 \cdot ID^{2.223}}\right]^{0.5} \quad (18)$$

This work was supported by a grant of the Deutsche Forschungsgemeinschaft.

Received 22 July 1985; accepted in final form 8 July 1986.

REFERENCES

1. ALBRECHT, K. H., P. GAEHTGENS, A. R. PRIES, AND M. HEUSER. The Fahraeus effect in narrow capillaries (i.d. 3.3 to 11.0 μm). *Microvasc. Res.* 18: 33–47, 1979.
2. BARBEE, J. H., AND G. R. COKELET. The Fahraeus effect. *Microvasc. Res.* 3: 6–16, 1971.
3. CHIEN, S., S. USAMI, AND R. SKALAK. Blood flow in small tubes. In: *Handbook of Physiology. The Cardiovascular System.* Bethesda, MD: Am. Physiol. Soc., 1984, sect. 2, vol. IV, pt. 1, chapt. 6, p. 217–249.
4. COKELET, G. R. Macroscopic rheology and tube flow of human blood. In: *Microcirculation,* edited by J. Grayson, and W. Zingg. New York: Plenum, 1976, vol. I, p. 9–31.
5. COKELET, G. R. Speculation on a cause of low vessel hematocrits in the microcirculation. *Microcirculation* 2: 1–18, 1982.
6. DELLIMORE, J. W., M. J. DUNLOP, AND P. B. CANHAM. Ratio of cells and plasma in blood flowing past branches in small plastic channels. *Am. J. Physiol.* 244 (*Heart Circ. Physiol.* 13): H635–H643, 1983.
7. FAHRAEUS, R. Die Strömungsverhältnisse und die Verteilung der Blutzellen im Gefäßsystem. *Klin. Wochenschr.* 7: 100–106, 1928.
8. FENTON, B. M., R. T. CARR, AND G. R. COKELET. Nonuniform red cell distribution in 20 − 100 μm bifurcations. *Microvasc. Res.* 29: 103–126, 1985.
9. GAEHTGENS, P. Flow of blood through narrow capillaries: rheological mechanisms determining capillary hematocrit and apparent viscosity. *Biorheology* 17: 183–189, 1980.
10. GAEHTGENS, P., K. H. ALBRECHT, AND F. KREUTZ. Fahraeus effect and cell screening during tube flow of human blood. I. Effect of variation of flow rate. *Biorheology* 15: 147–154, 1978.
11. GAEHTGENS, P., K. LEY, AND A. R. PRIES. Topological approach to the analysis of microvessel network structure and hematocrit distribution. In: *Microvascular Networks: Experimental and Theoretical Studies,* edited by A. S. Popel and P. C. Johnson. Basel: Karger. In press.
12. GIBSON, J. G., A. M. SELIGMAN, W. C. PEACOCK, J. C. AUB, J. FINE, AND R. D. EVANS. The distribution of red cells and plasma in large and minute vessels of the normal dog, determined by radioactive isotopes of iron and iodine. *J. Clin. Invest.* 25: 848–857, 1946.
13. HEYMANN, M. A., B. D. PAYNE, J. I. E. HOFFMAN, AND A. M. RUDOLPH. Blood flow measurements with radionuclide-labeled particles. *Prog. Cardiovasc. Dis.* 20: 55–79, 1977.
14. HORTON, R. E. Erosional development of streams and their drainage basins; hydrophysical approach to quantitative morphology. *Bull. Geol. Soc. Am.* 56: 275–370, 1945.
15. HOUSE, S. D., AND H. H. LIPOWSKY. Distribution of microvessel hematocrit and blood flow in cremaster muscle (Abstract). *Microvasc. Res.* 29: 225, 1985.
16. JOHNSON, P. C. Red cell separation in the mesenteric capillary network. *Am. J. Physiol.* 221: 99–104, 1971.
17. JOHNSON, P. C., J. BLASCHKE, K. S. BURTON, AND J. H. DIAL. Influence of flow variations on capillary hematocrit in mesentery. *Am. J. Physiol.* 221: 105–112, 1971.
18. KANZOW, G., A. R. PRIES, AND P. GAEHTGENS. Analysis of the hematocrit distribution in the mesenteric microcirculation. *Int. J. Microcirc.: Clin. Exp.* 1: 67–79, 1982.
19. KLITZMAN, B., AND B. R. DULING. Microvascular hematocrit and red cell flow in resting and contracting striated muscle. *Am. J. Physiol.* 237 (*Heart Circ. Physiol.* 6): H481–H490, 1979.
20. KLITZMAN, B., AND P. C. JOHNSON. Capillary network geometry and red cell distribution in the hamster cremaster muscle. *Am. J. Physiol.* 242 (*Heart Circ. Physiol.* 11): H211–H219, 1982.
21. LIPOWSKY, H. H., S. USAMI, AND S. CHIEN. In vivo measurements of "apparent viscosity" and microvessel hematocrit in the mesentery of the cat. *Microvasc. Res.* 19: 297–319, 1980.
22. MICHEL, C. C. Fluid movement through capillary walls. In: *Handbook of Physiology. The Cardiovascular System.* Bethesda, MD: Am. Physiol. Soc., 1984, sect. 2, vol. IV, pt. 1, chapt. 9, p. 375–409.
23. POPEL, A. S. Effect of heterogeneity of capillary flow on the capillary hematocrit. *Proc. Am. Soc. Mech. Eng. Appl. Mech. Div.* 32: 83–84, 1979.
24. PRIES, A. R., K. H. ALBRECHT, AND P. GAEHTGENS. Model studies on phase separation at a capillary orifice. *Biorheology* 18: 355–367, 1981.
25. PRIES, A. R., P. GAEHTGENS, AND G. KANZOW. Microvascular distribution of blood volume flow and hematocrit as related to oxygen delivery. *Adv. Physiol. Sci.* 25: 291–300, 1981.
26. PRIES, A. R., G. KANZOW, AND P. GAEHTGENS. Microphotometric determination of hematocrit in small vessels. *Am. J. Physiol.* 245 (*Heart Circ. Physiol.* 14): H167–H177, 1983.
27. SCHMID-SCHÖNBEIN, G. W., R. SKALAK, S. USAMI, AND S. CHIEN. Cell distribution in capillary networks. *Microvasc. Res.* 19: 18–44, 1980.
28. SCHMID-SCHÖNBEIN, G. W., AND B. W. ZWEIFACH. RBC velocity profiles in arterioles and venules of the rabbit omentum. *Microvasc. Res.* 10: 153–164, 1975.
29. SLAAF, D. W., R. ALEWIJNSE, AND H. WAYLAND. Use of telescopic imaging in intravital microscopy: a simple solution for conventional microscopes. *Int. J. Microcirc. Clin. Exp.* 1: 121–134, 1982.
30. STRAHLER, A. N. Hypsometric (area altitude) analysis of erosional topology. *Bull. Geol. Soc. Am.* 63: 1117–1142, 1952.
31. YEN, R. T., AND Y. C. FUNG. Effect of velocity distribution on red cell distribution in capillary blood vessels. *Am. J. Physiol.* 235 (*Heart Circ. Physiol.* 4): H251–H257, 1978.